SLAC-PUB-1770
July 1976
(E)

INELASTIC ELECTRON DEUTERON SCATTERING IN THE THRESHOLD REGION AT HIGH MOMENTUM TRANSFER*

W. P. Schütz, R. G. Arnold, B. T. Chertok, E. B. Dally, **
A. Grigorian, †† C. L. Jordan, ‡ and R. Zdarko††

American University§
Washington, D. C. 20016

F. Martin

Stanford Linear Accelerator Center
Stanford University, Stanford, California 94305

B. A Mecking

Physikalisches Institut
Universität Bonn, Bonn, West Germany

ABSTRACT

At squared momentum transfers $0.8 \leq q^2 \leq 6.0\ (\mathrm{GeV}/c)^2$, we measured nine spectra of inelastic electron deuteron scattering cross sections in the threshold region between 0 and 2.3% in $\Delta p/p$ below the elastic peak and deduced the deuteron inelastic structure function νW_2. We found $\nu W_2(\omega')$ approaching a universal scaling curve and a close relation between νW_2 and the deuteron elastic structure function $A(q^2)$.

(Submitted to Phys. Rev. Letters.)

---

*Work supported in part by the Energy Research and Development Administration.

**On leave from Naval Postgraduate School, Monterey, California 93940.
††Present address: High Energy Physics Laboratory, Stanford University, Stanford, California 94305.
‡Present address: LeCroy Research Systems Corp., 1 First Street, Los Altos, California 94022.
§Research supported by the National Science Foundation under Grant No. MPS 75-07325.

In this letter, we report preliminary results of inelastic electron deuteron scattering in the threshold region at high momentum transfer q. The data were taken from a SLAC experiment[1] whose main purpose was to measure the elastic scattering cross sections and the deuteron structure function $A(q^2)$ at nine values of q^2 in the region $0.8 \leq q^2 \leq 6.0$ $(\mathrm{GeV/c})^2$. The experimental conditions were such that we measured not only the elastic events, but also inelastic events from deuteron breakup and pion production between $0 \geq \Delta p/p_e \geq -2.3\%$, where p_e is the scattered electron momentum at the center of the elastic peak. The nine inelastic electron spectra span an unusual dynamic region of large q^2 and small energy transfer $\nu = E_i - E_f$, the difference between initial and final electron energy. This region has not been explored before. Bjorken scaling is expected when both q^2 and ν are large compared with M_N^2, the square of the nucleon mass, as in deep inelastic electron scattering. The data presented here are on a scale where q^2 is expected to resolve the nucleons into fermion quark currents while ν is typical of excitation energies where nucleon-nucleon final state interaction effects may be significant. The deuteron, then, is an ideal system to study the approach to scaling and the interplay between nuclear and particle physics.

We used the 20 GeV/c spectrometer of SLAC End Station A to detect scattered electrons at a fixed $\theta_e = 8^\circ$ from liquid deuterium, liquid hydrogen (for system calibration) and from a dummy target to determine the empty target background. To filter the elastic events out of the inelastic and background events, we used the 8 GeV/c spectrometer in coincidence with the 20 GeV/c spectrometer to detect the recoil deuterons with elastic kinematics.

The 20 GeV/c spectrometer with 5% momentum acceptance was set to cover the region in Δp between $-.03 \leq \Delta p/p_e \leq +.02$. Events from the electron arm were logged when a coincidence signal in three scintillator trigger counters and a large pulse height in a lead glass and lead lucite shower counter was registered. Thus, simultaneous with the double arm elastic events, we recorded single arm events from inelastic processes in the threshold region.

Five planes of multiwire proportional chambers recorded the particle trajectory at the spectrometer exit. The angle and momentum of the particles leaving the target were reconstructed using the well-known optical properties of the spectrometer.

A typical electron spectrum is shown in Fig. 1 displaying the total spectrum and the elastic and empty target background events. Subtracting the background and elastic events from the total spectrum gives us the inelastic events we want to investigate here. The finite resolution, mainly caused by the initial electron beam momentum spread, is roughly 0.5% of p_e and given by the width of the elastic peak.

Figure 2 shows the kinematic region of our nine spectra on a q^2-ν-plane. The dotted line indicates the experimental limit at 2.3% of p_e below the center of the elastic peak. The pion threshold is always inside, the center of the quasi-elastic peak always outside the spectra.

For radiative unfolding, we used a method suggested by Crannell[2] using the radiative correction formulas given by Tsai.[3] This gave an enhancement to the spectra of typically a factor 1.8 with very little energy dependency. The solid angle $\Delta\Omega$ was determined in a Monte Carlo simulation. Experimental corrections were applied for dead time losses (5 to 10%) and for wire chamber track inefficiencies (10%).

Our results for the inelastic cross sections $d^2\sigma/d\Omega dE_f$ versus E_f are presented in Fig. 3. The error bars on the data points represent the statistical errors only. The systematical errors, mainly from uncertainties in $\Delta\Omega$ and the corrections, are estimated to ±20%. The spectra rise almost exponentially with decreasing E_f, with a sharp rise from zero at the threshold.

The influence of the resolution on the shape of the spectra at threshold was studied by folding the resolution into faked "true" spectra. This study indicated that the "true" spectra apparently rise from zero with nonzero slope. Thus, the threshold enhancement cannot be explained as a resolution effect. It is possible that it is caused by final state interactions between the outgoing proton and neutron which have small relative momentum.

In one photon exchange approximation, the cross section can be written as

$$\frac{d^2\sigma}{d\Omega dE_f} = \frac{\sigma_M}{\nu} \cdot \left[\nu W_2(q^2,\nu) + \nu W_1(q^2,\nu) \cdot \tan^2\frac{\theta_e}{2}\right]$$

where σ_M is the Mott cross section and W_1 and W_2 are the deuteron inelastic structure functions, depending on the Lorentz invariants q^2 and ν. Formulas connecting W_1 and W_2 are given, e.g., in Ref. 4. Assuming $R = 0.18$,[5] we find for our case

$$\nu W_1 \cdot \tan^2\frac{\theta_e}{2} / \nu W_2 \leq .011$$

which means that we are practically only sensitive to νW_2. For q^2, $\nu \rightarrow \infty$, it is observed that νW_2 becomes a function of the scaling variable ω' only, with $\omega' = 1 + W^2/q^2$ and $W^2 = M^2 + 2M\nu - q^2$, the square of the missing mass. Figure 4 shows a comparison of our data with data from Refs. 5 and 7 on a νW_2 vs. ω' plot.[6] At q^2 below 2 $(GeV/c)^2$, we are not yet in the scaling region, but at $q^2 \geq 2$ $(GeV/c)^2$, our spectra merge with increasing q^2 into a universal $\nu W_2(\omega')$ curve. We find empirically that the spectra with $q^2 \geq 2$ $(GeV/c)^2$ can be described by the relation $\nu W_2 \sim (\omega' - 0.5)^n$, with $n = 6 \pm 0.5$.

We find a close relation between the elastic $A(q^2)$ and W_2 at constant W^2. $A(q^2)$ is observed to approach the power-law behavior $F_d = \sqrt{A} \sim (q^2)^{-5}$ (see Ref. 1) as predicted by Brodsky and Farrar's dimensional-scaling quark model.[8] Using the form

$$F_d \sim F_p^2(q^2/4) \cdot \left(1 + \frac{q^2}{\frac{6}{5} m^2}\right)^{-1} \tag{1}$$

with $F_p = (1+q^2/.71)^{-2}$ and $m^2 = .47/2\ \mathrm{GeV}^2$ (see Ref. 9) the onset of scaling was observed to be already below $q^2 = 0.8\ (\mathrm{GeV/c})^2$.

For W (Ref. 6) close to M_d, we find empirically that our data follow the relation

$$W_2 \sim F_d^2(q^2) \cdot \rho(W^2) \tag{2}$$

with F_d given by Eq. (1) and a function ρ only depending on W^2 (see Fig. 5).

A connection between F and νW_2 near threshold has been given by Drell-Yan[10] and West[11] for the case of the proton:

$$\nu W_2 \sim x \cdot (1-x)^p , \quad F \sim (1/q^2)^{(p+1)/2} , \quad x = \frac{q^2}{2M\nu} \to 1 .$$

If we extend this prediction to the deuteron, we postulate p=9, since $F \sim (1/q^2)^5$. From our data, we could not get a reasonable fit within $4 \leq p \leq 11$. So, we do not have any evidence that this connection works for the deuteron. However, we seem to be at too small q^2, ν-values to observe scaling in x.

If $G(q^2)$ is the excitation form factor of a resonance at $M=M_R$,

$$\nu W_2 = \left(M_R^2 - M_d^2 + q^2\right) \cdot \left[G(q^2)\right]^2 \cdot \delta\left(W^2 - M_R^2\right)$$

is its contribution to νW_2 in the narrow resonance approximation. This has been shown by Bloom and Gilman.[12] Our data indicate that this relation works in our case ($M_R \approx M_d$), i.e., $\nu W_2 \sim q^2 \cdot F_d^2 \cdot \rho(W^2)$, similar to Eq. (2). Thus, our measurements indicate that νW_2 at threshold behaves like a resonance with $G(q^2) \sim F_d(q^2)$. This leads, in the language of the quark model, to the conclusion that, like in the elastic case, all six quarks participate in the threshold inelastic scattering process.

We thank Dr. S. Brodsky for many helpful suggestions and discussions.

REFERENCES

1. R. Arnold et al., Phys. Rev. Letters 35, 776 (1975).
2. H. Crannell, Nucl. Instr. Meth. 71, 208 (1969).
3. P. Tsai, Stanford Linear Accelerator Center preprint SLAC-PUB-848 (1971).
4. S. Stein et al., Phys. Rev. D 12, 1884 (1975).
5. J. S. Poucher et al., Phys. Rev. Letters 32, 118 (1974).
6. For comparison with Refs. 5 and 7, we calculated W^2 with $M_N = .938$ GeV. Our data are then in the range $-2.12 \leq W^2 \leq 0.76$ GeV^2. For comparison of νW_2 with F_d, we defined W^2 with $M_d = 1.876$ GeV ($3.52 \leq W^2 \leq 5.02$ GeV^2).
7. E. M. Riordan, thesis, MIT Report No. COO-3069-176.
8. S. Brodsky and G. Farrar, Phys. Rev. D 11, 1309 (1975).
9. S. Brodsky and B. Chertok, to be published.
10. S. D. Drell and T. M. Yan, Phys. Rev. Letters 24, 181 (1970).
11. G. B. West, Phys. Rev. Letters 24, 1206 (1970).
12. E. D. Bloom and F. J. Gilman, Phys. Rev. Letters 25, 1140 (1970).

FIGURE CAPTIONS

1. Electron events at $q^2 = 1\ (\mathrm{GeV}/c)^2$.

2. Kinematic region of this experiment.

3. Inelastic cross sections versus final electron energy.

4. Our data compared with results from Refs. 5 ($\theta = 6^\circ,\ 10^\circ$; $W > 2$ GeV; $q^2 > 1\ (\mathrm{GeV}/c)^2$) and 7 ($\theta = 18^\circ,\ 26^\circ,\ 34^\circ$; $W \geq 2$ GeV; $q^2 \geq 4\ (\mathrm{GeV}/c)^2$).

5. Inelastic structure function W_2 divided by the elastic structure function A at constant missing mass. $F_d = A^{1/2}$. The lines are eyeball fits.

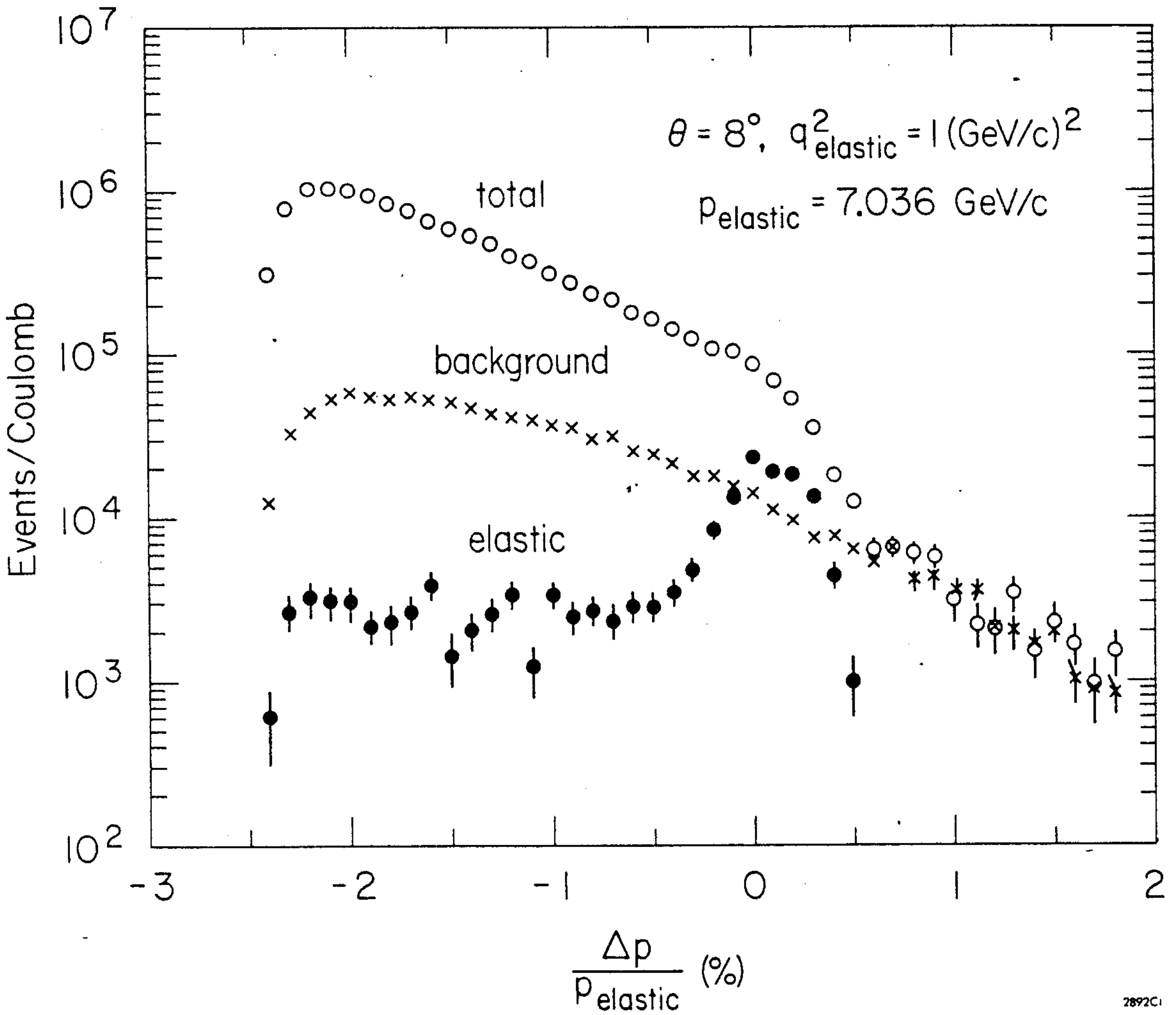

$\theta = 8°$, $q^2_{elastic} = 1\,(GeV/c)^2$
$p_{elastic} = 7.036$ GeV/c
total
background
elastic
Events/Coulomb
10^7
10^6
10^5
10^4
10^3
10^2
-3
-2
-1
0
1
2
$\frac{\Delta p}{p_{elastic}}$ (%)
2892C1

Fig. 1

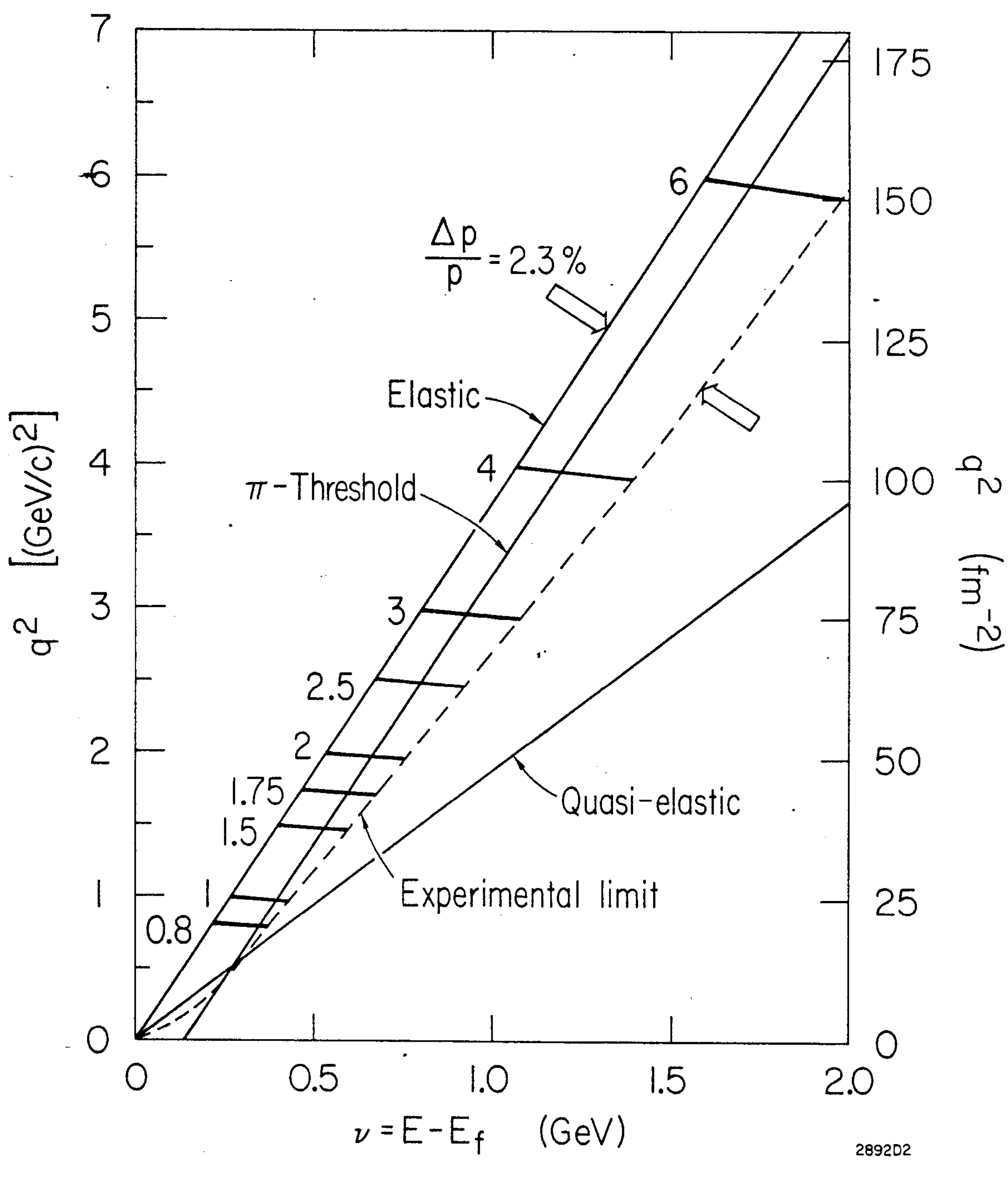

$\frac{\Delta p}{p} = 2.3\%$
Elastic
π-Threshold
Quasi-elastic
Experimental limit
6
4
3
2.5
2
1.75
1.5
1
0.8
q^2 [(GeV/c)^2]
q^2 (fm^{-2})
$\nu = E - E_f$ (GeV)
0
0.5
1.0
1.5
2.0
1
2
3
4
5
6
7
25
50
75
100
125
150
175
2892D2

Fig. 2

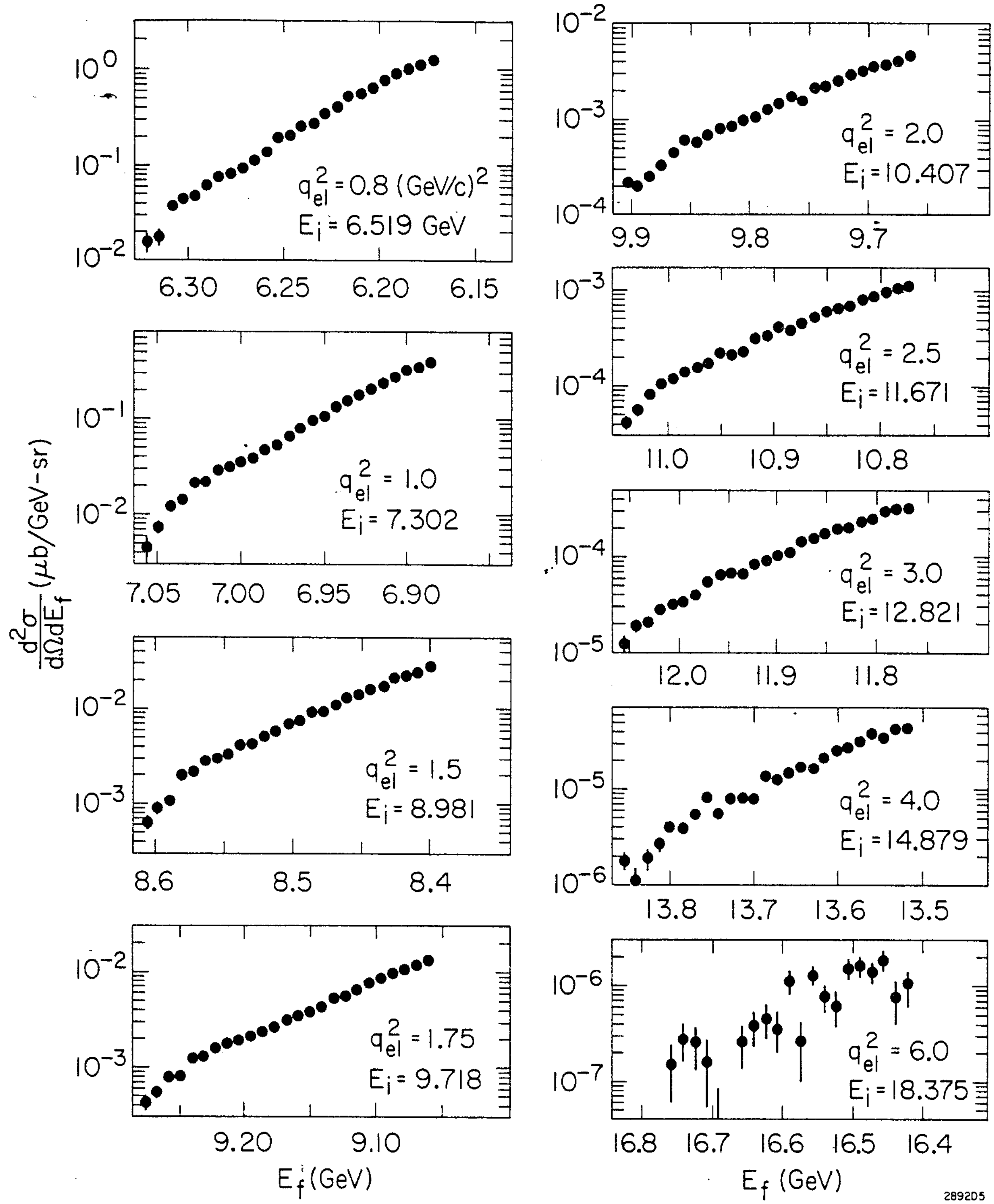

$\frac{d^2\sigma}{d\Omega dE_f}$ (μb/GeV-sr)
q_{el}^2 = 0.8 (GeV/c)^2
E_i = 6.519 GeV
q_{el}^2 = 1.0
E_i = 7.302
q_{el}^2 = 1.5
E_i = 8.981
q_{el}^2 = 1.75
E_i = 9.718
q_{el}^2 = 2.0
E_i = 10.407
q_{el}^2 = 2.5
E_i = 11.671
q_{el}^2 = 3.0
E_i = 12.821
q_{el}^2 = 4.0
E_i = 14.879
q_{el}^2 = 6.0
E_i = 18.375
E_f (GeV)
E_f (GeV)
289205

Fig. 3

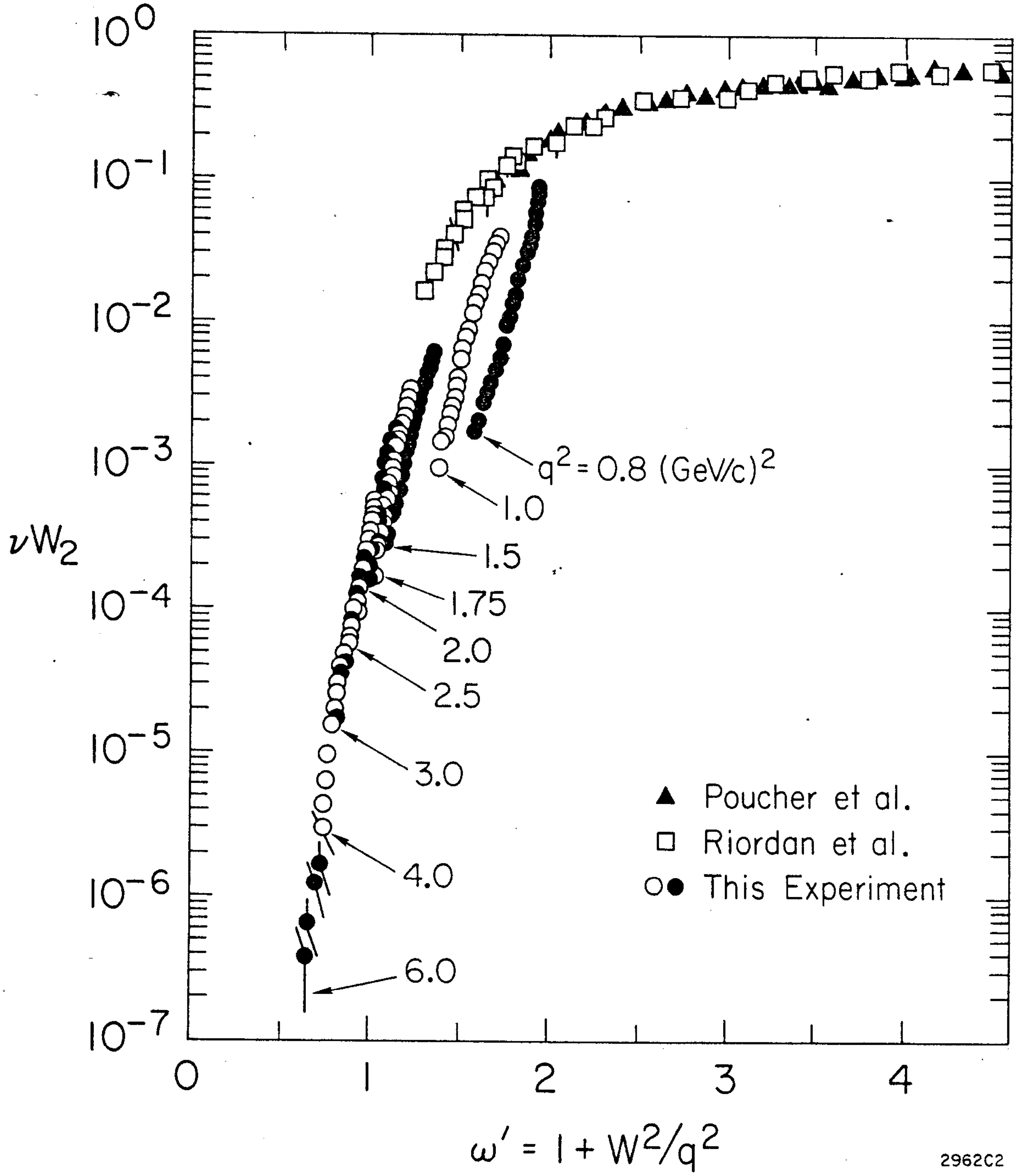

10^0
10^{-1}
10^{-2}
10^{-3}
10^{-4}
10^{-5}
10^{-6}
10^{-7}
νW_2
$q^2 = 0.8\ (GeV/c)^2$
1.0
1.5
1.75
2.0
2.5
3.0
4.0
6.0
Poucher et al.
Riordan et al.
This Experiment
0
1
2
3
4
$\omega' = 1 + W^2/q^2$
2962C2

Fig. 4

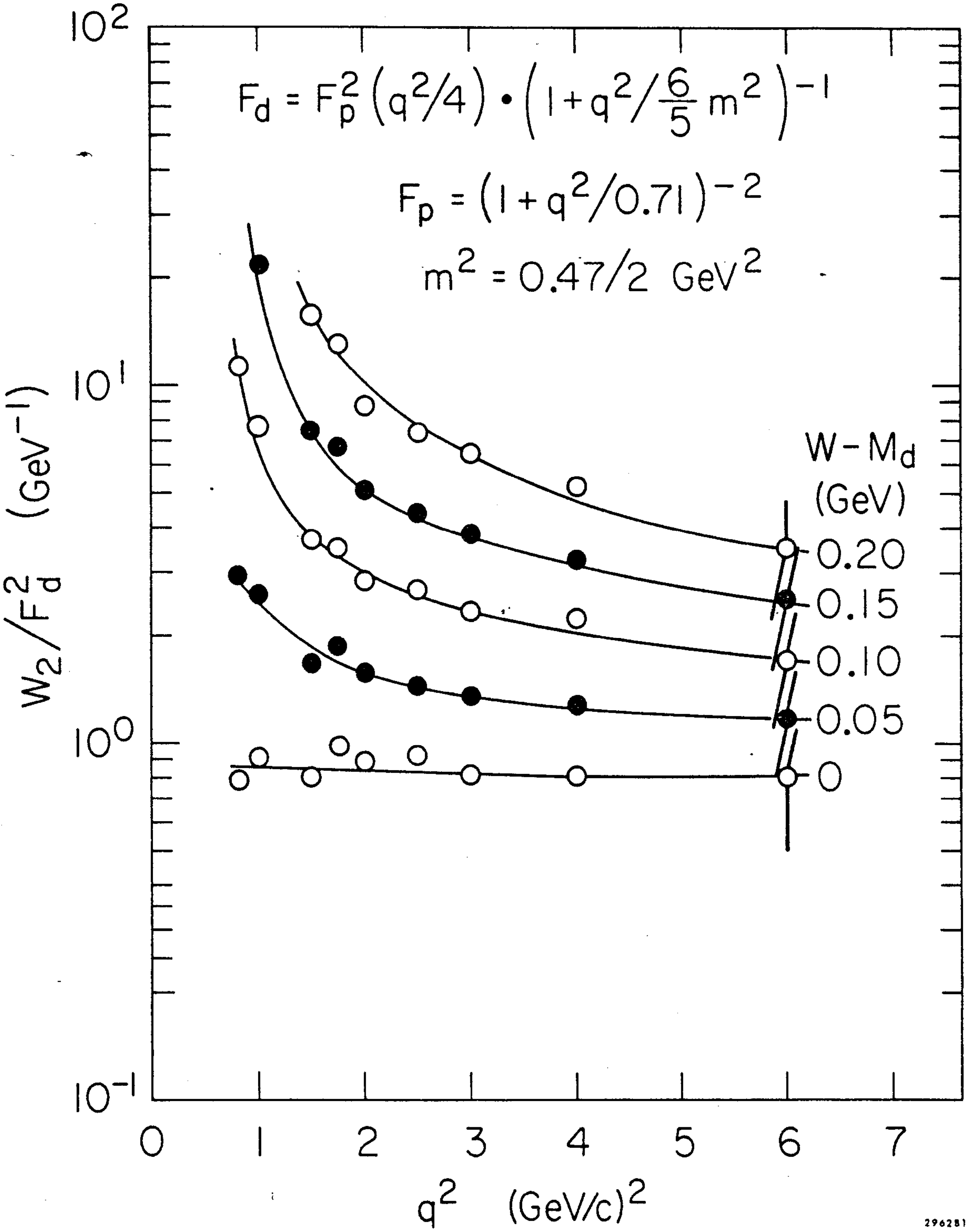

$F_d = F_p^2(q^2/4) \bullet \left(1+q^2/\frac{6}{5}m^2\right)^{-1}$
$F_p = (1+q^2/0.71)^{-2}$
$m^2 = 0.47/2\ \mathrm{GeV}^2$
$W - M_d$
(GeV)
0.20
0.15
0.10
0.05
0
10^2
10^1
10^0
10^{-1}
W_2/F_d^2 (GeV^{-1})
0
1
2
3
4
5
6
7
q^2 $(\mathrm{GeV/c})^2$
296281

Fig. 5